Check for updates

Research Article Vol. 26, No. 23 | 12 Nov 2018 | OPTICS EXPRESS 30116

Optics EXPRESS

Definition of a measurement scale of graininess from reflectance and visual measurements

A. FERRERO,[1,*] J. L. VELÁZQUEZ,[1] E. PERALES,[2] J. CAMPOS,[1] AND F. M. MARTÍNEZ VERDÚ[2]

[1] *Instituto de Óptica "Daza de Valdés" (IO, CSIC), Agencia Estatal CSIC, C/ Serrano 121, 28006 Madrid, Spain*
[2] *Color & Vision Group, University of Alicante, Carretera de San Vicente del Raspeig s/n, 03690 Alicante, Spain*
[*] *alejandro.ferrero@csic.es*

Abstract: Effect pigments in coatings produce eye-catching colour and texture effects and are widely used in automotive, cosmetics, coatings, inks, flooring, textile or decoration. One of these texture effects is graininess, which is the perceived texture exhibited when the effect coating is observed under diffuse illumination. To date there is not a standard procedure to measure graininess from reflectance measurements. The objective of this work is to propose a methodology for traceable graininess measurements, similarly as it was proposed for colour in 1931. In this article, the relevant reflectance-based quantities are clearly defined, and a formal relation with data from visual experiments is given. This methodology would allow a measurement scale of graininess and a difference formula to be agreed once conclusive visual data become available.

1. Introduction

The use of effect pigments has allowed new eye-catching visual effects in products [1–5]. Unlike the traditional absorption pigments, they can generate appearance impressions extremely angle dependent, both on the illumination and observation directions. As a consequence of their appealing appearances, the market of effect pigments is steadily increasing and they have become very popular in automotive, cosmetics, coatings, inks, flooring, textile or decoration. The visual effects introduced by the use of these effect pigments must be somehow quantified by spectrophotometric, image capturing/processing and visual methods, and standards must be developed in order to provide with traceability to industry, since these effects are paramount for the quality of products. Effect pigments are embedded in a material or binder to compose an "effect coating". Its visual effect is determined by the optical properties of material and effect pigments, but also by their concentration, size and orientation in the material. Two visual textures can be observed in many cases. One is referred as sparkle, or glint, among other terms, and it is observed under directional illumination as point light sources distributed on a dark surround, similarly as stars on the night sky or the Sun's glitter on the sea [6]. Sparkle is produced because the effect pigments behave as isolated microscopic mirrors, not perfectly aligned with respect to the surface of the sample, which is key for this visual texture [7]. Texture of effect coatings, as colour, depends strongly on the illumination and observation directions. As a consequence, texture depend also strongly on the solid angle of illumination, because the reflected luminous flux is averaged over a bunch of directions [7, 8]. Then, sparkle disappears toward larger solid angles, and, at the extreme case of diffuse illumination, a second kind of visual texture can be observed, a granular appearance usually named graininess or diffuse coarseness [9]. It must be noticed that, although this work was motivated for characterising effect coatings, both visual textures can be observed in other micro–structured surfaces, as for example in displays, when using anti-glare layers [10].

#340151 https://doi.org/10.1364/OE.26.030116
Journal © 2018 Received 24 Jul 2018; revised 23 Aug 2018; accepted 25 Aug 2018; published 1 Nov 2018

Optics EXPRESS

The present technological state of imaging technology allows both sparkle and graininess to be quantified, but until recently the only commercially–available instrument able to quantify sparkle and graininess had been BYK-mac, which provides three sparkle indexes (area, intensity and general) for three geometries (incidence angles at 15º, 45º and 75º, and a fixed collection angle at 0º), and one graininess index. These indexes are supposedly well-correlated with the visual experience. However, their corresponding measurands are not clearly defined and, therefore, they cannot be measured by other instruments. Recently, the company X-Rite has introduced two new portable multiangle spectrophotometers in the market (MA-T6 and MA-T12), which can quantify sparkle and graininess too. BYK-mac and the two X-Rite multiangle-spectrophotometers have their own sparkle and graininess scales, because to date there is not a standard procedure to obtain sparkle and graininess correlates from reflectance-related measurements. In consequence, the indexes provided by these instruments are not traceable to international standards, and impossible to be reproduced by National Metrology Institutes (NMI) or other companies, which need to develop their own scales.

The objective of this work is to define the material's reflectance-based quantities that are relevant to the perception of graininess and can be correlated with data from visual experiments. We propose a methodology that includes the measurement procedure of luminance factor images, the method to calculate the reflected–based quantities from these images, and an equation able to link reflectance and visual data by fitting. Real graininess samples are used in this study, whose visual textures are representative of those observed in effect coatings, so that they may be used as visual scale. This study would allow the measurement scale of graininess and the difference formula to be agreed once conclusive visual data become available.

In his generalization of the colorimetric approach to texture, Richards showed that any arbitrary spatial stimuli could be matched mixing four or six primaries, depending if eye movements are allowed or not [11]. This dimensionality can be reduced in situations where there is a lawful relationship between the contributions at various scales [12]. According to several works [13–16], a reasonable fractal-based model for the amplitude spectra of many natural spatiotemporal textures is:

$$A(f_s, f_t) = K f_s^{-\alpha_s} f_t^{-\alpha_t}, \tag{1}$$

where f_s and f_t are spatial and temporal frequencies, respectively, and being K, α_t and α_s constants [12]. Billock et al. [12] proposed an appearance map of the dynamic texture space, analogously to the CIE 1931 colour space [17], using as coordinates the α_t and α_s exponents, and determining their Just-Noticeable Differences, analogously to MacAdam's ellipses in colorimetry [18]. It suggests that only a single dimension is required to describe the spatial distribution of graininess. These and other works suggest that a Fourier-transform approach is fundamental for the quantification of graininess, as it was already applied in [19].

2. Samples and experimental setup

2.1. Graininess samples

A set of 25 achromatic graininess samples (8 cm × 13 cm) was used in this study (see the picture in Fig. 1). They belong to the Effect Navigator set produced by Standox. Each sample is labelled with a L number and an EN number, both of them varying from 1 to 5, whose permutation makes the total 25 samples. We know by private communication that the L number is related to the concentration of effect pigments, whereas the EN number is related to the average size of the pigments. Therefore, in this paper, L is denoted as "Pigment concentration Id." and EN as "Pigment size Id.". The graininess sample set can be regarded as five groups of samples with fixed concentration of pigments and variable pigment sizes, or, reciprocally, as five groups of fixed pigment sizes and a variable concentration of pigments. We know that the larger the pigment concentration Id., the lower the concentration of pigments, and that the larger the pigment size

Optics EXPRESS

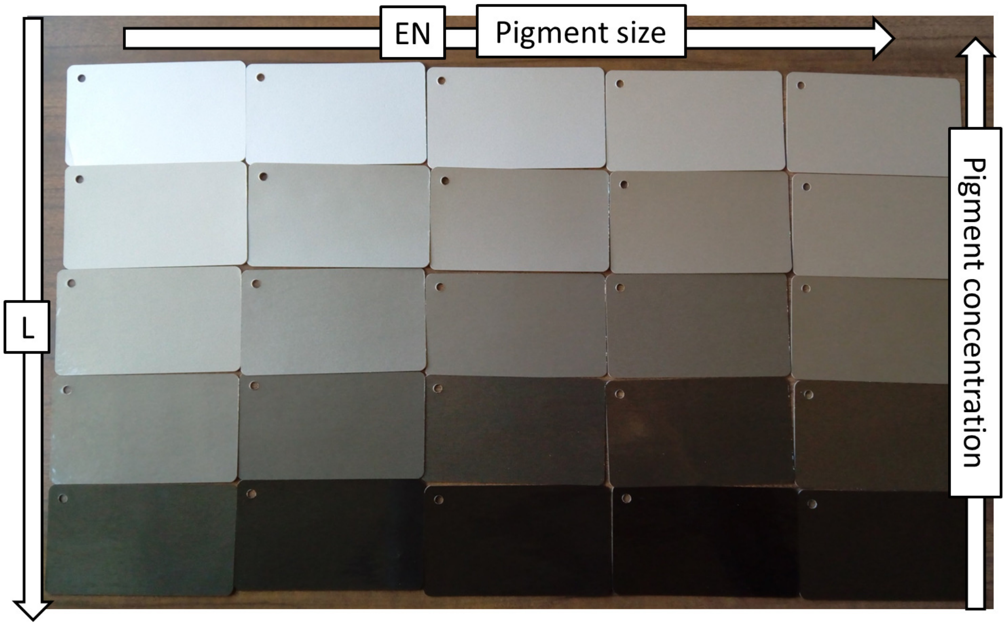

Fig. 1. Set of 25 graininess samples (8 cm × 13 cm) used in this study.

Id., the larger the average size of the pigments, but we do not know the exact relation between these identification numbers and the real values. Visually, it is quite evident that the larger the pigment concentration Id., the lighter the sample, which means that the reflectance is related to the concentration of pigments. This set of samples is representative enough to be used as visual scale for graininess.

2.2. Experimental setup and reflectance measurement

Since a surface can present graininess only when it is illuminated by diffuse light (diffuse illumination) an integrating sphere was used as illumination source (Fig. 2). It was a 50.8 cm in diameter integrating sphere coated with Spectraflect, externally illuminated by a white phosphor-based LED with CCT = 3225 K (its spectral power distribution is shown at Fig. 3) through a 2.5 cm in diameter port (source port), at a distance of 4 cm to avoid direct illumination on the sample, which is located at a 5 cm in diameter port (sample port) 90^{o} apart from the source port. The illuminance on the samples is around 100 lx. The graininess images are acquired by a camera located at a port opposite to the sample port (camera port, 12.5 cm in diameter), so that frontal images are acquired. The high quality camera has a 1/2″ Sony ICX414AL CCD sensor, with squared pixels (9.9 μm×9.9 μm). Its photoresponse non-uniformity (PRNU) is 0.3% under white light. A Navitar Zoom 7000 18:108 mm objective zoom lens was used with a f-number of 2.5, which provides a scale pixel factor of 45.8 μm/pixel ± 0.6 μm/pixel at the working distance.

The described set-up intends to acquire the relevant reflectance-based quantities required to find graininess correlates. A similar set-up can be used to measure graininess once a standard graininess observer is defined.

Thirty subsequent images (**I**) were acquired and averaged for each graininess sample under the described conditions, along with dark images (**D**). Images of a white ceramic diffuse reflectance standard (**W**) were acquired in the same way. **I** and **W** are acquired exactly at the same conditions of illumination and collection, whereas **D** is acquired in absence of sample, with the room in completely dark conditions, but with the source on, so the dark image includes the stray light into

Optics EXPRESS

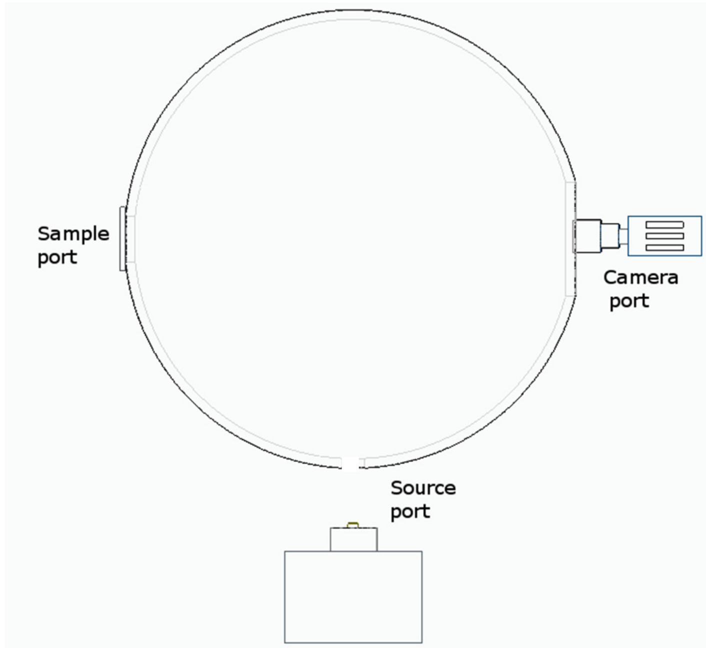

Fig. 2. Experimental set-up for the reflectance measurement.

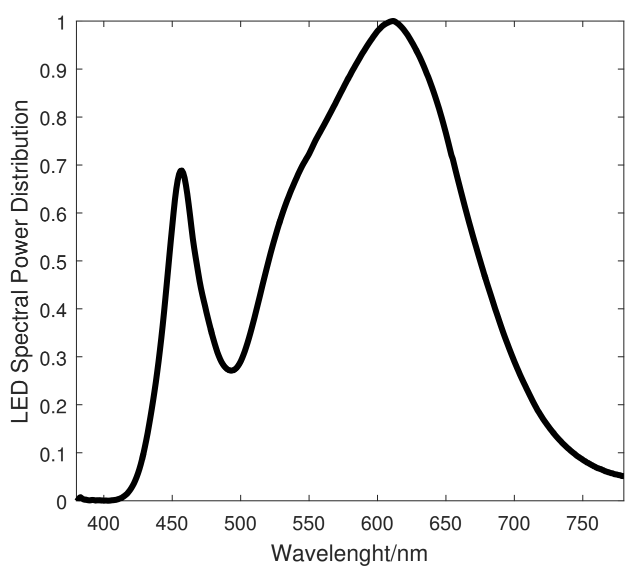

Fig. 3. Spectral power distribution of the phosphor-based LED used as light source in Fig. 2.

Optics EXPRESS

the camera from the sphere. **W** is used to provide an absolute value of the luminance factor to each graininess sample, but also to compensate the non-uniformity introduced by the camera objective lens. Both absolute value assignment and non-uniformity compensation are accomplished by calculating the graininess images (**R**) from (**I**) according to the following equation:

$$R_{ij} = \frac{I_{ij} - D_{ij}}{W_{ij} - D_{ij}} \times R_{\mathrm{W}} \tag{2}$$

where R_{ij}, I_{ij}, D_{ij} and W_{ij} are the values of the (i,j)-pixels in images **R**, **I**, **D** and **W**, respectively, and R_{W} is the luminance factor value of the white diffuse reflectance standard. Although R_{W} is considered independent of the pixel, the surface of the white diffuse reflectance standard is not completely uniform. There are some small-scale defects in the images of **W**, typically, less than 10% decreases of reflectance on less than about 0.4 mm. It is not certainly an issue when these standards are used for common reflectance calibrations, where a comparatively much larger measurement area is defined. However, since these defects may interfere with the spatial analysis of graininess, they were smoothed before using Eq. (2) by a moving average filter on the image with span of 123 pixels.

Three complete measurements were done for each sample to account the reproducibility when slightly different areas of the samples are used. An average variation of 1.2% in the pixels value was obtained. The data shown in this text correspond with means of the three measurements.

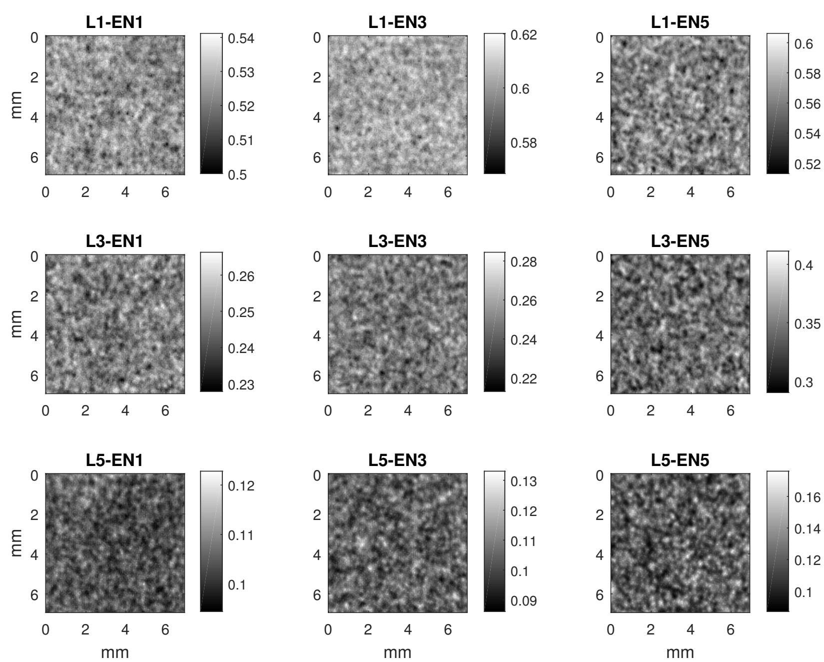

Fig. 4. Graininess images (**R**) of a reduced set of samples (those with odd pigment concentration and size Ids.). Only a squared and centered region of interest of 6.9 mm × 6.9 mm (151 pixels × 151 pixels) is shown. The grey bars represent the luminance factor values of the pixels.

It must be noticed that the values of the pixels in the images **I**−**D** and **W**−**D** are spectrally integrated values of the product of the spectral power distribution of the light source (S) (see

Fig. 3), the spectral responsivity of the camera (s), the reflectance factor of the coating of the integrating sphere (R_{is}) and the reflectance factor of the samples (R_{I}) or standard (R_{W}). If the measured quantities have to be correlated with visual data, it is convenient that the spectral responsivity of the camera matches the spectral luminous efficiency function for photopic vision, $V(\lambda)$, defined in ISO 23539:2005(E)/CIE S010/E:2004 [20]. Otherwise, a spectral mismatch correction factor needs to be applied to the ratio in Eq. (2), which can be calculated as:

$$F = \frac{W_{ij}/W_{ij,\text{V}}}{I_{ij}/I_{ij,\text{V}}} = \tag{3}$$

$$= \frac{\int_{360\text{ nm}}^{830\text{ nm}} S(\lambda)s(\lambda)R_{\text{is}}(\lambda)R_{\text{W}}(\lambda)\text{d}\lambda \int_{360\text{ nm}}^{830\text{ nm}} S(\lambda)V(\lambda)R_{\text{is}}(\lambda)R_{\text{I}}(\lambda)\text{d}\lambda}{\int_{360\text{ nm}}^{830\text{ nm}} S(\lambda)V(\lambda)R_{\text{is}}(\lambda)R_{\text{W}}(\lambda)\text{d}\lambda \int_{360\text{ nm}}^{830\text{ nm}} S(\lambda)s(\lambda)R_{\text{is}}(\lambda)R_{\text{I}}(\lambda)\text{d}\lambda}$$

where $I_{ij,\text{V}}$ and $W_{ij,\text{V}}$ are pixels' responses if their spectral responsivity of the camera were exactly $V(\lambda)$. F takes value 1 (no correction required) if R_{I}, R_{W} and R_{is} are spectrally neutral. It is assumed for white standards and integrating sphere coatings, and for the set of achromatic graininess samples used in this work. If the graininess samples were very chromatic, a $V(\lambda)$-filtered camera is recommended.

Conventional photometry, with the use of a photopic filter and applying the spectral mismatch correction factor [21], makes the results completely independent of the spectral power distribution of the light source. Notice that the mean spectral mismatch error from using the 3225 K LED source instead of light sources with spectral power distributions of CIE standards illuminants (A or D65) or other usual broadband illuminants is lower than 1% [22]. This error does not have noticeable impact on our results, and spectral mismatch correction is not necessary.

2.3. Graininess images

Graininess images (**R**) of a reduced set of samples (those with odd pigment concentration and size Ids.) are shown in Fig. 4. In order to clearly display the graininess appearance of the images, only a squared and centered region of interest (ROI) of 6.9 mm × 6.9 mm (151 pixels × 151 pixels) is shown. The images in the figure are arranged in a grid for which each column has constant average pigment size and each row constant pigment concentration. The values of the absolute luminance factor (R_{ij}) are given in grey code at the right of each figure. This value decreases considerably with the L number, or pigment concentration Id. On the other hand, the pigment size does not seem to have a noticeable impact on the apparent size of the grains, which are clearly visible.

3. Relevant reflectance-based quantities

3.1. Power spectral density of graininess images

Graininess may be described as spatially-correlated lightness variations on the surface, as the texture patterns shown in Fig. 4. To quantify graininess from these images, only the lightness variation at spatial frequencies related to the graininess must be accounted, which roughly are determined by the size of the grains.

In order to evaluate the spatial variations at different spatial frequencies, the Power Spectral Density (PSD) is calculated for each graininess sample, at the same ROI that the one selected for images in Fig. 4. The decimal logarithms of the PSDs for the samples with odd Ids., together with the PSD result of a white sample without graininess, are shown in Fig. 5 as a function of the spatial frequency in mm^{-1}. Isotropy is assumed, and the PSD is calculated as the average of the PSDs of columns and rows of the images.

For all the graininess samples, the amplitude spectrum follows a fractal-based model as in Eq. (1), with spatial exponent α_{s} around 0.4.

Optics EXPRESS

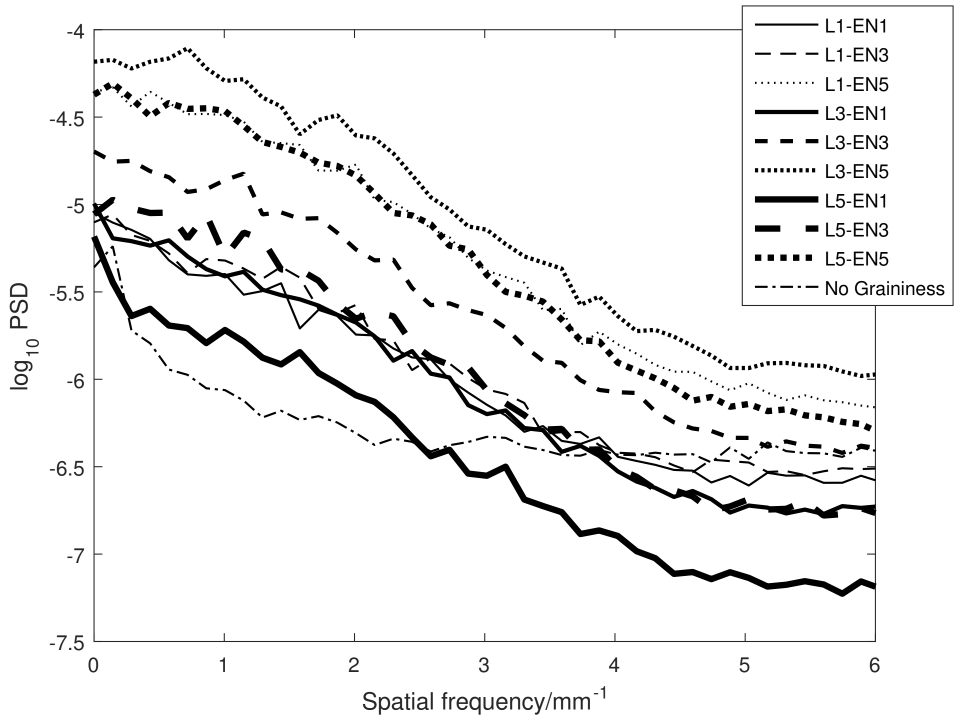

Fig. 5. Decimal logarithms of the PSDs for the samples with odd Ids., together with the PSD of a white sample without graininess ("No Graininess").

3.2. Graininess variance and average luminance factor

The integration of the PSD between frequencies of 0 mm^{-1} and the maximum spatial frequency corresponds to half the variance of the graininess image [23]. This variance quantifies the variation of the values regardless the spatial frequency. If integration is just done between frequencies f_1 and f_2, those variations at frequencies lower than f_1 and higher than f_2 are ignored. These two parameters can be determined to specifically quantify those variations associated to what it can be understood as graininess. Then, we propose here a first relevant reflectance-based quantity to quantify graininess, graininess variance (V_G), formally defined as:

$$V_G(f_1, f_2) = 2\int_{f_1}^{f_2} \text{PSD}(f)\text{d}f, \tag{4}$$

where f_1 and f_2 are parameters to be determined by correlation with visual data. The factor 2 is introduced to account the two symmetric sides of the Fourier Transform (single-sided amplitude spectrum). Notice that this quantity, as a variance, is closely related with the root-mean-square (RMS) calculation of image contrast C_{rms}, a good predictor of the relative/apparent contrast of compound grating images [24] and random noise patterns [25] [26].

For a given absolute spatial variation of the luminance of a surface, the inhomogeneity is better perceived the lower is the average luminance. After a close visual assessment of the samples, it appeared very evident that the lightness of the samples is relevant in the perception of graininess. For two samples with the same pigment size Id., the darker one always shows a higher graininess, although it may be also caused by the lower pigment concentration. Both the luminance and its spatial variation due to graininess are proportional to the illuminance on the surface, being the luminance factor the proportionality factor related to the sample. Then, the average luminance factor obtained for the samples (β, average of $R_{i,j}$) need to be considered to find correlation with visual data, and it is proposed as the second relevant reflectance-based quantity for the quantification of graininess.

4. Relation with structural values

It is expected that the defined reflectance-based quantities (V_G and β) are related with structural values (average pigment size and pigment concentration), and not only with the visual experience of graininess.

The relations with the structural values of the studied set of samples are shown in Fig. 6 (again, only for odd Ids.). On the left graph of the figure, the values of the average luminance factor are shown as a function of the pigment size Id. (X axis) and the pigment concentration Id. (different curves for each Id.). The average luminance factor varies in great extent with the pigment concentration, while has only a slight dependence on the pigment size. The higher the pigment concentration (lower Id. number), the larger the average luminance factor, and the lighter the sample appears. Similarly, the relation of the graininess variance (V_G) with structural values is shown on the right graph, where f_1 = 1.32 mm^{-1} and f_2 = 1.66 mm^{-1} were used for the calculation of V_G, as a result of the procedure that will be described here. In contrast to the average luminance factor, V_G has a clear dependence on the pigment size, and only a slight dependence on the pigment concentration. The larger the pigment size (higher Id. number), the larger V_G. A sample without graininess, as that whose PSD is shown in Fig. 5, has a V_G value of around $6{\times}10^{-4}$, less than two thirds the value of the graininess sample with the lowest V_G.

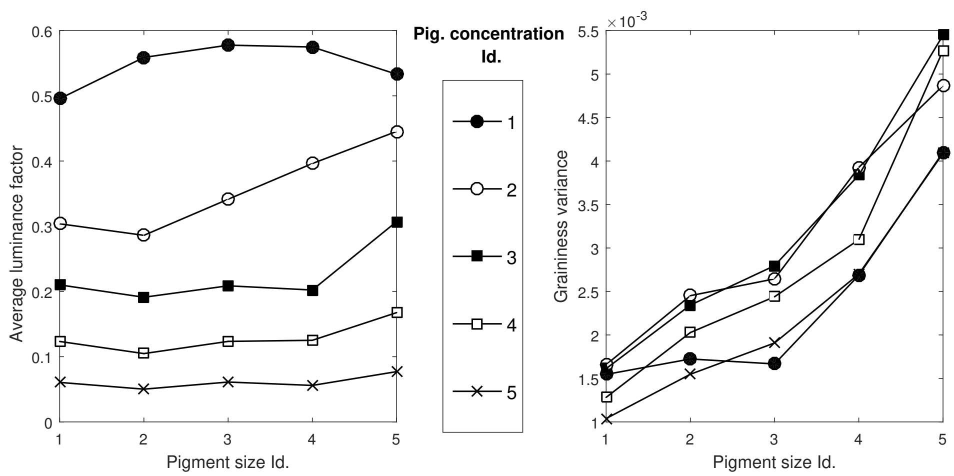

Fig. 6. Relation of the reflectance-based quantities with pigment concentration and size: (left graph) average luminance factor (β); (right graph) graininess variance (V_G).

5. A prospect of measurement scale of graininess

To define a measurement scale of graininess, visual data obtained by controlled visual experiments are required, which have to be mathematically related with the reflectance-based quantities defined in the previous section. To show the suitability of these quantities to be correlated with visual data, two tentative sets of visual data were used here. After close inspection of the data, the equation

$$G = V_G(f_1, f_2) \times (1 + \frac{a}{\beta^b}), \quad (5)$$

with f_1, f_2, a and b as free parameters, was found adequate to correlate both tentative visual data and the reflectance data here obtained, and therefore it will be used to quantify graininess.

The first tentative set of visual data consists of the graininess indexes acquired by the BYK-mac instrument for the graininess samples. These data can be regarded as visual data of G because this graininess index was developed considering visual experiments. The Eq. (5) could be fitted to these visual data with a linear correlation coefficient above 0.988, with fitting parameter values: $f_1 = 1.27$ mm^{-1}, $f_2 = 1.69$ mm^{-1}, $a = 0.12$, and $b = 0.84$. The obtained values of G for all studied samples, when Eq. (5) with those parameter values is used as graininess definition, are shown in Fig. 7(a). In the plot, where the X-axis and the Y-axis are the average luminance factor and the graininess variance, respectively, each white point represents a sample, identified with the correspondent L and EN numbers. The grey level expresses the graininess value G, according to the grey code in the bar at the right. This kind of representation allows structural (L and EN numbers), reflectance-based (V_G and β) and visual data (G) to be summed up in a single figure. Notice that the plot is limited by the most extreme values of V_G and β from the used set of samples, but it does not involve that results from any sample is restricted to those limits.

The second tentative set used as visual data for the studied samples was obtained at the University of Alicante (UA) from a preliminary visual experiment consisting of comparing samples with the same pigment concentrations but different pigment sizes. It was found that the Eq. (5) could be fitted to the present data with a linear correlation coefficient slightly above 0.97, by using as parameter values: $f_1 = 1.32$ mm^{-1}, $f_2 = 1.66$ mm^{-1}, $a = 0.14$, and $b = 1.14$, which are similar to those obtained with the first tentative set. The result for these visual data is represented in Fig. 7(b), analogously to Fig. 7(a). Since fitting parameters are similar, both figures look similar, and confirm a reasonable coherence of the two tentative sets of visual data. In addition, the figures show that, as expected, a high graininess variance and a low average luminance factor favour graininess perception, as it does a low pigment concentration (large L) and a large pigment size (large EN).

It must be remarked that the representations in Figs. 7(b) and 7(a) cannot be taken as a definitive graininess diagram, because more reliable data are required. However, given the similarity of both diagrams, and given the independence of the two tentative sets of visual data, it is expected that a very similar diagram may be taken as definitive in the future.

6. Discussion

The proposed methodology would allow graininess to be measured with traceability once a measurement scale of graininess is defined. The measurement scale of graininess would relate the reflectance-based quantities (average luminance factor and graininess variance) with the visual experience of graininess (visual data) by Eq. (5), with values f_1, f_2, a and b, which define a graininess standard observer and must be agreed using conclusive visual data. This standard observer may depend on the illuminance level on the sample, so it could be necessary to determine a standard illuminance level, for instance, that of an overcast day, which is a typical situation where graininess is observed. The dependence of the graininess on the illuminace level could be studied with a similar methodology that the one proposed here.

Once the measurement scale of graininess is defined, a graininess difference formula needs to be developed. Similarly to the case of colour, it can be defined to indicate imperceptible difference when the calculated difference is lower than 1. Billock et al. already studied the Just-Noticeable Differences of texture by considering the exponents of the spatial and temporal frequencies [see Eq. (1)] [12]. The spatial exponents for our data are always around 0.4, regardless the graininess sample. It corresponds with fine textures and it is precisely the exponent value for which spatial discriminations are harder, according to the same authors [12]. In this case, no correlation between these exponents and graininess was revealed. Notice that our aim is to quantify the perceived amount of a specific kind of texture (graininess) observed in samples, and not to

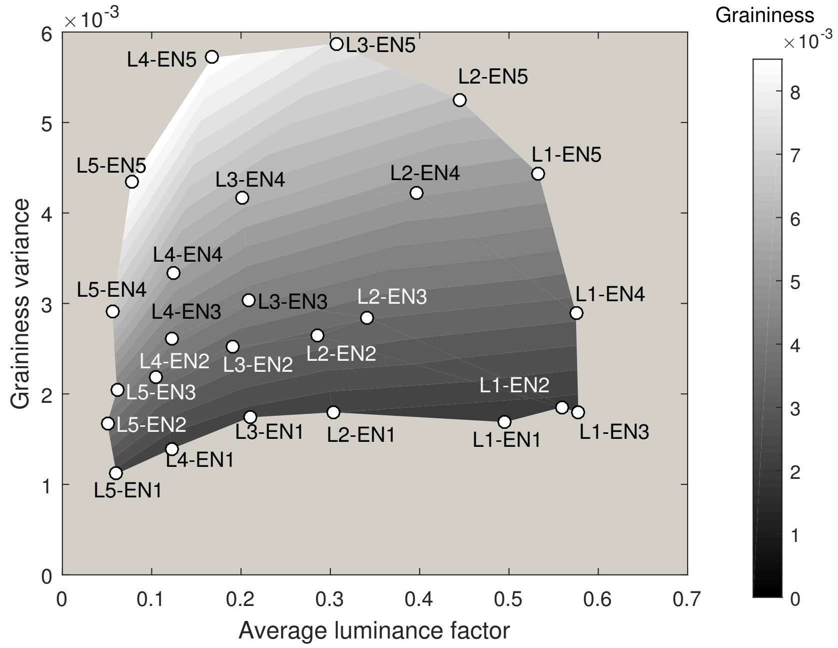

(a) BYK-mac.

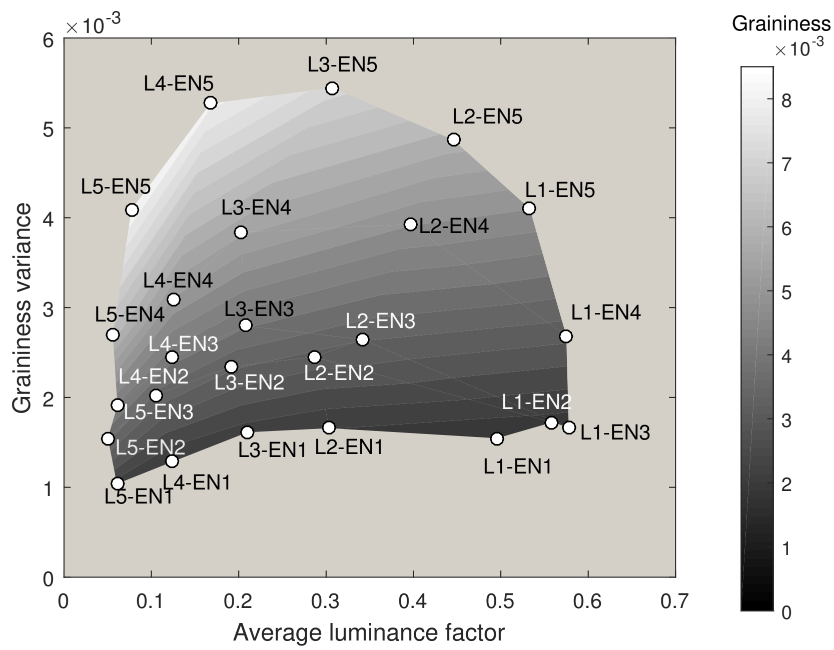

(b) UA.

Fig. 7. Representation of graininess using (a) BYK-mac's graininess index and (b) UA's visual data as visual data.

distinguish between different kinds of textures, as Billock et al. [12], and we do not think that the Billock's approach is enough in this case. For instance, the samples L1-EN5 and L5-EN5 present very different values of graininess (Fig. 7), but their PSD curves are almost identical within the relevant integration range (Fig. 5). For these two samples is absolutely obvious that the comparison of the PSD curves is not enough, and that the difference in graininess can only be predicted by taking into account the average luminance factors.

The results presented in this article indicate that the higher the concentration of effect pigments, the higher the average luminance factor, at least for the studied samples, and the lower the graininess, and that the larger the average size of the pigments, the higher the graininess. Both conclusions are coherent with the fact that graininess is, as sparkle, mainly produced by the proportion of light reflected by the effect pigments in the coating. According to this qualitative observation, it is expected that the variance graininess and the average luminance factor could be functionally related with the average pigment size and the pigment concentration. Then, graininess can be calculated using Eq. (5) for given values of these two structural variables.

The above proposed equation for graininess [Eq. (5)] ignores the dependence of graininess on the observer distance. But there are such dependence, since the contrast sensitivity of the human visual system depends on the spatial frequencies of the illuminance variation on the retina and not in the object plane. To consider this dependence, the contrast-sensitivity function (CSF) [27] may have been applied to weight Eq. (4) similarly as in [19]. We did not make use of it because the spatial frequencies involved in the observation at typical distances are around the maximum of the CSF, and we think that it would not affect notably the correlation with the visual data at any of those observation distances.

7. Conclusions

A methodology has been proposed for traceable graininess measurements. The results obtained for 25 graininess samples with different concentrations and sizes of pigments have been presented. The experimental setup for the reflectance and image-based measurements has been described. The average luminance factor, the power spectral density of the acquired graininess images, and the here defined graininess variance have been identified as the relevant reflectance-based quantities. The presented results indicate that the higher the concentration of effect pigments, the higher the average luminance factor, at least for the studied samples, and the lower the graininess; and that the larger the average size of the pigments, the higher the graininess. An equation to relate the reflectance-based quantities and, indirectly, the structural variables with the visual data of graininess has been proposed, and its performance has been showed for two tentative sets of visual data. However, more conclusive visual data are still required to define a definitive measurement scale of graininess and a graininess difference formula.

Funding

EURAMET and the European Union (16NRM08); Comunidad de Madrid (S2013/MIT-2790); Spanish Ministry of Economy and Competitiveness (DPI2015-65814-R).

Acknowledgments

This article was written within the EMPIR 16NRM08 Project "Bidirectional reflectance definitions" (BiRD). The EMPIR is jointly funded by the EMPIR participating countries within EURAMET and the European Union. Part of the authors (Instituto de Óptica "Daza de Valdés" (IO, CSIC), Agencia Estatal CSIC) are also grateful to Comunidad de Madrid for funding the project SINFOTON-CM: S2013/MIT-2790. Part of the authors (Color & Vision Group, University of Alicante) are also grateful to Spanish Ministry of Economy and Competitiveness for funding the project ADIREVGAO: DPI2015-65814-R.

References

1. G. A. Klein, *Industrial Color Physics*, vol. 154 (Springer, 2010).
2. H.-J. Streitberger and K.-F. Dossel, *Automotive Paints and Coatings* (Wiley-Vch, 2008).
3. E. B. Faulkner and R. J. Schwartz, *High Performance Pigments* (John Wiley & Sons, 2009).
4. F. J. Maile, G. Pfaff, and P. Reynders, "Effect pigments-past, present and future," Prog. organic coatings **54**, 150–163 (2005).
5. P. Wißling, *Metallic Effect Pigments: Fundamentals and Applications* (Vincentz Network GmbH & Co KG, 2006).
6. C. Cox and W. Munk, "Measurement of the roughness of the sea surface from photographs of the sun's glitter," JOSA **44**, 838–850 (1954).
7. A. Ferrero, J. Campos, A. M. Rabal, and A. Pons, "A single analytical model for sparkle and graininess patterns in texture of effect coatings," Opt. Express **21**, 26812–26819 (2013).
8. S. Ershov, A. Khodulev, and K. Kolchin, "Simulation of sparkles in metallic paints," (1999), pp. 121–128.
9. E. Kirchner, G. J. van den Kieboom, L. Njo, R. Sùper, and R. Gottenbos, "Observation of visual texture of metallic and pearlescent materials," Col. Res. Appl. **32**, 256–266 (2007).
10. M. E. Becker, "Sparkle measurement revisited: A closer look at the details," J. Soc. for Inf. Disp. **23**, 472–485 (2015).
11. W. Richards, "Quantifying sensory channels: generalizing colorimetry to orientation and texture, touch, and tones," Sens. Process. **3**, 207–229 (1979).
12. V. A. Billock, D. W. Cunningham, P. R. Havig, and B. H. Tsou, "Perception of spatiotemporal random fractals: an extension of colorimetric methods to the study of dynamic texture," JOSA A **18**, 2404–2413 (2001).
13. A. Pentland, *Fractal-based Descriptions of Surfaces* (MIT Press, 1988).
14. D. J. Field, "Relations between the statistics of natural images and the response properties of cortical cells," JOSA A **4**, 2379–2394 (1987).
15. D. Tolhurst, Y. Tadmor, and T. Chao, "Amplitude spectra of natural images," Ophthalmic Physiol. Opt. **12**, 229–232 (1992).
16. V. A. Billock, "Neural acclimation to 1/f spatial frequency spectra in natural images transduced by the human visual system," Phys. D: Nonlinear Phenom. **137**, 379–391 (2000).
17. J. Schanda, *Colorimetry: Understanding the CIE System* (John Wiley & Sons, 2007).
18. D. L. MacAdam, "Visual sensitivities to color differences in daylight," JOSA **32**, 247–274 (1942).
19. S. Kitaguchi, M. R. Luo, E. J. Kirchner, and G.-J. van den Kieboom, "Computational model for perceptual coarseness prediction," in "Conference on Colour in Graphics, Imaging, and Vision," (Society for Imaging Science and Technology, 2006), pp. 278–282.
20. "ISO Standard: ISO 23539:2005(E)/CIE S010/E:2004 ," in "Photometry - The CIE system of physical photometry," (2004).
21. R. Rattunde and P. Blattner, "CIE International Standard: CIE S 023/E:2013," in "Characterization of the Performance of Illuminance Meters and Luminance Meters," (CIE, 2013).
22. A. Kokka, T. Poikonen, P. Blattner, S. Jost, A. Ferrero, T. Pulli, M. Ngo, A. Thorseth, T. Gerloff, P. Dekker *et al.*, "Development of white LED illuminants for colorimetry and recommendation of white LED reference spectrum for photometry," Metrologia **55**, 526 (2018).
23. R. B. Blackman and J. W. Tukey, *The Measurement of Power Spectra* (Dover Publications, 1958).
24. K. Tiippana, R. Näsänen, and J. Rovamo, "Contrast matching of two-dimensional compound gratings," Vis. Res. **34**, 1157–1163 (1994).
25. B. Moulden, F. Kingdom, and L. F. Gatley, "The standard deviation of luminance as a metric for contrast in random-dot images," Perception **19**, 79–101 (1990).
26. P. J. Bex and W. Makous, "Spatial frequency, phase, and the contrast of natural images," JOSA A **19**, 1096–1106 (2002).
27. F. W. Campbell and J. Robson, "Application of Fourier analysis to the visibility of gratings," J. Physiol. **197**, 551–566 (1968).